

Acoustic scattering theory without large-distance asymptotics

Chi-Chun Zhou,^a Wen-Du Li,^{b,a} and Wu-Sheng Dai^{a*}

^a*Department of Physics, Tianjin University, Tianjin 300350, P.R. China*

^b*Theoretical Physics Division, Chern Institute of Mathematics, Nankai University, Tianjin, 300071, P. R. China*

ABSTRACT: In conventional acoustic scattering theory, a large-distance asymptotic approximation is employed. In this approximation, a far-field pattern, an asymptotic approximation of the exact result, is used to describe a scattering process. The information of the distance between target and observer, however, is lost in the large-distance asymptotic approximation. In this paper, we provide a rigorous theory of acoustic scattering without the large-distance asymptotic approximation. Moreover, as examples, we consider acoustic scattering on a rigid sphere and on a nonrigid sphere. We also illustrate the influence of the near target effect on the angular distribution of outgoing waves. It is shown that for long wavelength acoustic scattering, the near target effect must be reckoned in.

KEYWORDS: Acoustic scattering; Large-distance asymptotics; Near target effect.

*daiwusheng@tju.edu.cn.

Contents

1	Introduction	1
2	Acoustic scattering theory without large-distance asymptotics	2
2.1	Exact pattern	2
2.2	Scattering phase shift	3
2.3	Scattering intensity and sound pressure	4
3	Acoustic scattering on rigid sphere	5
3.1	Scattering intensity	5
3.2	Near target effect	6
3.3	Power	6
4	Acoustic scattering on nonrigid sphere	7
4.1	Scattering intensity	7
4.2	Near target effect	11
4.3	Power	12
5	Discussions and conclusion	12

1 Introduction

Solving an acoustic scattering problem boils down to solving a Helmholtz equation

$$(\nabla^2 + k^2) u(\mathbf{x}) = 0 \quad (1.1)$$

with a given boundary condition, where k is the wave number and $u(\mathbf{x})$ describes the complex amplitude of acoustic pressures [1–4]. If the incident wave is a plane wave, the solution of Eq. (1.1) can be written as

$$u(\mathbf{x}) = e^{i\mathbf{k}\cdot\mathbf{x}} + u^s(\mathbf{x}), \quad (1.2)$$

where \mathbf{k} is the wave vector of the incident wave and $u^s(\mathbf{x})$ is the outgoing wave [2–4]. Then the task of solving $u(\mathbf{x})$ is converted into solving the outgoing wave $u^s(\mathbf{x})$.

In conventional acoustic scattering theory, the outgoing wave $u^s(\mathbf{x})$ is approximately solved under a large-distance asymptotics [2–4]:

$$u^s(\mathbf{x}) = \frac{e^{ik|\mathbf{x}|}}{|\mathbf{x}|} u_\infty\left(\frac{\mathbf{x}}{|\mathbf{x}|}\right) + O\left(\frac{1}{|\mathbf{x}|^2}\right), \quad (1.3)$$

where $u_\infty\left(\frac{\mathbf{x}}{|\mathbf{x}|}\right)$ is the far-field pattern of the outgoing wave. Then, instead of the exact outgoing wave $u^s(\mathbf{x})$, one turns to calculate the far-field pattern $u_\infty\left(\frac{\mathbf{x}}{|\mathbf{x}|}\right)$.

The large-distance asymptotic approximation supposes that the distance between target and observer is infinite. Obviously, such an approximation loses the information of the distance. As a result, the observable quantity, such as the scattering intensity $I(\mathbf{x})$, depends only on the angle of emergence.

In realistic acoustic scattering, however, the wavelength of acoustic waves is often comparable with the distance between target and observer. In long wavelength acoustic-wave scattering, the large-distance asymptotic approximation is not accurate enough and a scattering theory without large-distance asymptotics is needed.

Recently, a rigorous scattering theory without large-distance asymptotics in quantum mechanics is developed [5, 6]. In this scattering theory, the information of the distance between target and observer is taken into account, since there is no large-distance asymptotic approximation. Taking advantage of this rigorous scattering theory, in this paper, we develop a rigorous acoustic scattering theory without large-distance asymptotic approximation.

Acoustic scattering deals with the propagation of sounds. There are many researches on acoustic scattering, for example, acoustic waves scattering on different targets such as fluid spheroids [7] and finite rigid plates [8]. Underwater acoustic scattering is also an important issue, such as underwater acoustic scattering signal separation [9], acoustic scattering from underwater elastic objects [10], acoustic scattering by suspended flocculating sediments [11] and acoustic scattering in gassy soft marine sediments [12]. Different methods such as the time domain sampling method [13], the unsupervised machine learning method [14], and the numerical method [15] are investigated. Other problems such as acoustic scattering-resonance [16], acoustic scattering reductions [17], acoustic scattering in nonuniform potential flows [18], designing the bilaminate acoustic cloak [19], control of acoustic absorptions [20], acoustic interaction forces [21], acoustic radiation forces [22], and scattering effects on an acoustic black hole [23] are also considered.

In section 2, we construct an rigorous acoustic scattering theory without large-distance asymptotics. In sections 3 and 4, we consider two acoustic scattering processes, plane waves scattering on a rigid sphere and on a nonrigid sphere. The conclusion is summarized in section 5.

2 Acoustic scattering theory without large-distance asymptotics

As mentioned above, in conventional acoustic scattering theory, instead of the outgoing wave $u^s(\mathbf{x})$, one turns to find the far-field pattern $u_\infty\left(\frac{\mathbf{x}}{|\mathbf{x}|}\right)$, the large-distance asymptotic approximation of $u^s(\mathbf{x})$. In this section, instead of the far-field pattern $u_\infty\left(\frac{\mathbf{x}}{|\mathbf{x}|}\right)$, we calculate the exact result of the outgoing wave $u^s(\mathbf{x})$ by introducing an exact pattern $u_{exact}(\mathbf{x})$ which is an exact version of the far-field pattern $u_\infty\left(\frac{\mathbf{x}}{|\mathbf{x}|}\right)$.

2.1 Exact pattern

Introduce the exact pattern $u_{exact}(\mathbf{x})$ by rewriting the outgoing wave $u^s(\mathbf{x})$ in Eq. (1.2) as

$$u^s(\mathbf{x}) = \frac{e^{ik|\mathbf{x}|}}{|\mathbf{x}|} u_{exact}(\mathbf{x}). \quad (2.1)$$

As will be shown later, the exact pattern $u_{exact}(\mathbf{x})$ recovers the far-field pattern as $|\mathbf{x}|$ goes to infinity:

$$u_{exact}(\mathbf{x}) \stackrel{|\mathbf{x}| \rightarrow \infty}{\sim} u_{\infty}\left(\frac{\mathbf{x}}{|\mathbf{x}|}\right). \quad (2.2)$$

Now we represent the scattering intensity by the exact pattern $u_{exact}(\mathbf{x})$.

The scattering intensity $I(\mathbf{x})$ can be represented in terms of the exact pattern $u_{exact}(\mathbf{x})$ as

$$I(\mathbf{x}) = \frac{\rho_0 \omega k}{|\mathbf{x}|^2} |u_{exact}(\mathbf{x})|^2, \quad (2.3)$$

where ρ_0 is the density of the medium, ω is the frequency of the acoustic wave, and $k = 2\pi/\lambda$ with λ the wavelength.

Proof. The scattering intensity $I(\mathbf{x})$ is defined as the component of the energy flow in the radial direction,

$$I(\mathbf{x}) = \mathbf{J}_s(\mathbf{x}) \cdot \mathbf{e}_r, \quad (2.4)$$

where the energy flow $\mathbf{J}(\mathbf{x})$ is defined as [1, 2]

$$\mathbf{J}(\mathbf{x}) = \frac{1}{2} \frac{i}{\omega \rho_0} [u(\mathbf{x}) \nabla u^*(\mathbf{x}) - u^*(\mathbf{x}) \nabla u(\mathbf{x})]. \quad (2.5)$$

Substituting Eq. (2.1) into Eqs. (2.5) and (2.4) proves Eq. (2.3). ■

2.2 Scattering phase shift

In acoustic scattering, the target plays the role of the potential in quantum-mechanical scattering. In this section, we introduce the scattering phase shift δ_l and express the exact pattern $u_{exact}(\mathbf{x})$ in terms of the scattering phase shift.

The phase shift δ_l . The solution of Eq. (1.1) can be written as a linear combination of the spherical Hankle function [3, 6]

$$u(\mathbf{x}) = \sum_{l=0}^{\infty} C_l h_l^{(2)}(k|\mathbf{x}|) P_l(\cos \theta) + \sum_{l=0}^{\infty} D_l h_l^{(1)}(k|\mathbf{x}|) P_l(\cos \theta), \quad (2.6)$$

where $h_l^{(1)}(x)$ and $h_l^{(2)}(x)$ are the spherical Hankle functions of first and second kinds and $P_l(x)$ is the Legendre function.

The scattering phase shift δ_l is introduced as [6]

$$e^{2i\delta_l} = \frac{D_l}{C_l}. \quad (2.7)$$

The exact pattern $u_{exact}(\mathbf{x})$. Now we express the exact pattern $u_{exact}(\mathbf{x})$ explicitly in terms of the scattering phase shift δ_l .

The exact pattern $u_{exact}(\mathbf{x})$ can be represented in terms of the phase shift δ_l as

$$u_{exact}(\mathbf{x}) = \frac{1}{2ik} \sum_{l=0}^{\infty} (2l+1) \left(e^{2i\delta_l} - 1 \right) P_l(\cos \theta) y_l \left(-\frac{1}{ik|\mathbf{x}|} \right), \quad (2.8)$$

where $y_l(x) = \sum_{k=0}^l \frac{(l+k)!}{k!(l-k)!} \left(\frac{x}{2}\right)^k$ is the Bessel polynomial.

Proof. By the expression of the outgoing wave Eq. (2.1), the solution of the Helmholtz equation Eq. (1.2) can be written as

$$u(\mathbf{x}) = e^{ik|\mathbf{x}|\cos\theta} + \frac{e^{ik|\mathbf{x}|}}{|\mathbf{x}|} u_{exact}(\mathbf{x}). \quad (2.9)$$

The plane wave $e^{ik|\mathbf{x}|\cos\theta}$ in Eq. (2.9) can be exactly expanded as [6]

$$e^{ik|\mathbf{x}|\cos\theta} = \sum_{l=0}^{\infty} (2l+1) i^l M_l \left(-\frac{1}{ik|\mathbf{x}|} \right) \frac{1}{k|\mathbf{x}|} \sin \left[k|\mathbf{x}| - \frac{l\pi}{2} + \Delta_l \left(-\frac{1}{ik|\mathbf{x}|} \right) \right] P_l(\cos\theta), \quad (2.10)$$

where $M_l(x) = |y_l(x)|$ and $\Delta_l(x) = \arg y_l(x)$ are the modulus and argument of the Bessel polynomial $y_l(x)$. Substituting Eq. (2.10) into Eq. (2.9) gives

$$u(\mathbf{x}) = \sum_{l=0}^{\infty} (2l+1) i^l M_l \left(-\frac{1}{ik|\mathbf{x}|} \right) \frac{1}{k|\mathbf{x}|} \sin \left[k|\mathbf{x}| - \frac{l\pi}{2} + \Delta_l \left(-\frac{1}{ik|\mathbf{x}|} \right) \right] P_l(\cos\theta) + \frac{e^{ik|\mathbf{x}|}}{|\mathbf{x}|} \sum_{l=0}^{\infty} u_{exact}^{(l)}(\mathbf{x}), \quad (2.11)$$

where $u_{exact}(\mathbf{x})$ is expressed as

$$u_{exact}(\mathbf{x}) = \sum_{l=0}^{\infty} u_{exact}^{(l)}(\mathbf{x}). \quad (2.12)$$

Eq. (2.6) can be expressed as [6]

$$u(\mathbf{x}) = \sum_{l=0}^{\infty} A_l M_l \left(-\frac{1}{ik|\mathbf{x}|} \right) \frac{1}{k|\mathbf{x}|} \sin \left[k|\mathbf{x}| - \frac{l\pi}{2} + \delta_l + \Delta_l \left(-\frac{1}{ik|\mathbf{x}|} \right) \right] P_l(\cos\theta), \quad (2.13)$$

where $A_l = 2\sqrt{C_l D_l}$.

Rewriting the trigonometric function in Eqs. (2.11) and (2.13) in terms of the exponential function and equalling the coefficients of $e^{\pm ik|\mathbf{x}|}$ give

$$A_l = \frac{1}{2} i^l (2l+1) e^{i\delta_l} \quad (2.14)$$

and

$$u_{exact}^{(l)}(\mathbf{x}) = \frac{1}{2ik} (2l+1) \left(e^{2i\delta_l} - 1 \right) P_l(\cos\theta) y_l \left(-\frac{1}{ik|\mathbf{x}|} \right). \quad (2.15)$$

Substituting Eq. (2.15) into Eq. (2.12) proves Eq. (2.8). ■

2.3 Scattering intensity and sound pressure

The scattering intensity $I(\mathbf{x})$ in Eq. (2.3) is represented by the exact pattern $u_{exact}(\mathbf{x})$ and the exact pattern $u_{exact}(\mathbf{x})$ in Eq. (2.8) is represented by the phase shift δ_l . In this section, we represent the scattering intensity $I(\mathbf{x})$ and the pressure $p(\mathbf{x}, t)$ in terms of the phase shift δ_l .

The scattering intensity can be obtained by substituting Eq. (2.8) into Eq. (2.3):

$$I(\mathbf{x}) = \frac{\rho_0 \omega k}{|\mathbf{x}|^2} \left| \sum_{l=0}^{\infty} (2l+1) \frac{1}{2k} \left(e^{2i\delta_l} - 1 \right) y_l \left(-\frac{1}{ik|\mathbf{x}|} \right) P_l(\cos \theta) \right|^2. \quad (2.16)$$

The sound pressure $p(\mathbf{x}, t)$ is

$$p(\mathbf{x}, t) = \text{Re} [u(\mathbf{x}) e^{-i\omega t}], \quad (2.17)$$

where $u(\mathbf{x})$ is given by Eqs. (2.13) and (2.14). Then we have

$$p(\mathbf{x}, t) = \frac{\cos \omega t}{2k|\mathbf{x}|} \sum_{l=0}^{\infty} M_l \left(-\frac{1}{ik|\mathbf{x}|} \right) i^l (2l+1) e^{i\delta_l} \sin \left[k|\mathbf{x}| - \frac{l\pi}{2} + \delta_l + \Delta_l \left(-\frac{1}{ik|\mathbf{x}|} \right) \right] P_l(\cos \theta). \quad (2.18)$$

3 Acoustic scattering on rigid sphere

In this section, as an example, we consider the problem of a plane wave scattering on a rigid sphere.

3.1 Scattering intensity

The phase shift δ_l of a plane wave scattered by a rigid sphere can be obtained from the boundary condition. The boundary condition of a rigid sphere is [1, 4]

$$\frac{1}{i\omega\rho_0} \nabla u(\mathbf{x}) \Big|_{|\mathbf{x}|=a} = 0, \quad (3.1)$$

where a is the radius of the sphere. Substituting Eq. (2.6), $D_l = \frac{1}{4}i^l(2l+1)e^{2i\delta_l}$, and $C_l = \frac{1}{4}i^l(2l+1)$ [6] into the boundary condition (3.1) gives

$$\begin{aligned} e^{2i\delta_l} &= -\frac{dh_l^{(2)}(kr)/dr \Big|_{r=a}}{dh_l^{(1)}(kr)/dr \Big|_{r=a}} \\ &= \frac{\frac{l}{ka}h_l^{(2)}(ka) - h_{l+1}^{(2)}(ka)}{\frac{l}{ka}h_l^{(1)}(ka) - h_{l+1}^{(1)}(ka)}, \end{aligned} \quad (3.2)$$

where $\frac{d}{dz}h_\nu^{(1,2)}(z) = \frac{\nu}{z}h_\nu^{(1,2)}(z) - h_{\nu+1}^{(1,2)}(z)$ is used [24]. The phase shift, by noting that $h_l^{(2)*}(z) = h_l^{(1)}(z)$, then reads

$$\delta_l = \arg \left(\frac{l}{ka}h_l^{(2)}(ka) - h_{l+1}^{(2)}(ka) \right). \quad (3.3)$$

The scattering intensity then can be achieved by substituting Eq. (3.2) into Eq. (2.16):

$$I(\mathbf{x}) = \frac{\rho_0 \omega k}{|\mathbf{x}|^2} \left| \sum_{l=0}^{\infty} (2l+1) \frac{1}{2k} \left[\exp \left(2i \arg \left(\frac{l}{ka}h_l^{(2)}(ka) - h_{l+1}^{(2)}(ka) \right) \right) + 1 \right] y_l \left(-\frac{1}{ik|\mathbf{x}|} \right) P_l(\cos \theta) \right|^2. \quad (3.4)$$

Rayleigh scattering. Taking only the s -wave and p -wave contributions into account and assuming that $ka \ll 1$, we arrive at

$$I(\mathbf{x}) \sim \frac{\rho_0 \omega k^5 a^6}{9 |\mathbf{x}|^2} \left(1 - \frac{3}{2} \cos \theta\right)^2 \left[1 + \frac{1}{k^2 |\mathbf{x}|^2} \left(\frac{3 \cos \theta}{2 - 3 \cos \theta}\right)^2\right], \quad (3.5)$$

where $y_0\left(-\frac{1}{ik|\mathbf{x}|}\right) = 1$ and $y_1\left(-\frac{1}{ik|\mathbf{x}|}\right) = 1 - \frac{1}{ik|\mathbf{x}|}$ are used. One can see that the scattering intensity $I(\mathbf{x})$ is a function of both the angle θ and the distance $|\mathbf{x}|$. When $|\mathbf{x}| \rightarrow \infty$, $I(\mathbf{x})$ reduces to the result of the large-distance asymptotic approximation in conventional acoustic scattering theory [1, 4]:

$$I_\infty(\mathbf{x}) \sim \frac{\rho_0 \omega k^5 a^6}{9 |\mathbf{x}|^2} \left(1 - \frac{3}{2} \cos \theta\right)^2. \quad (3.6)$$

3.2 Near target effect

The large-distance asymptotic approximation in conventional scattering theory loses the information of the distance between target and observer. In the following, we show the influence of the near target effect in scattering cross sections.

The differential scattering cross section is given by [4]

$$\frac{d\sigma}{d\Omega} = I(\mathbf{x}) \frac{|\mathbf{x}|^2}{\rho_0 \omega k}, \quad (3.7)$$

where the scattering intensity $I(\mathbf{x})$ is given by Eq. (3.4). In figures (1) to (4), we illustrate $\left(\frac{d\sigma}{d\Omega}\right)^{1/2}/a$ versus the polar angle θ at different distance $|x|$ for different wave lengths up to the f -wave contribution.

From the figures we can see that the near target effect can not be ignored when the distance is comparable with the wave length. The exact result recovers the large-distance asymptotics in conventional scattering theory as the distance goes to infinity.

In order to show the near target effect, we consider the deviation $\Delta\sigma = \sigma - \sigma_\infty$. By Eqs. (3.7), (3.5), and (3.6), we have

$$\frac{d\Delta\sigma}{d\Omega} = \frac{k^2 a^6}{4 |\mathbf{x}|^2} \cos^2 \theta. \quad (3.8)$$

where we take only the s -wave and p -wave contributions into account and assume that $ka \ll 1$.

3.3 Power

The power of an acoustic scattering on a sphere can be calculated by [1, 4]

$$P_{sc} = \int_0^{2\pi} \int_0^\pi I(\mathbf{x}) |\mathbf{x}|^2 \sin \theta d\theta d\phi. \quad (3.9)$$

Substituting Eq. (3.5) into Eq. (3.9) gives

$$P_{sc}(\omega, \mathbf{x}) \sim \frac{7\pi \rho_0 \omega a^6 k^5}{9} \left(1 + \frac{3}{7k^2 |\mathbf{x}|^2}\right). \quad (3.10)$$

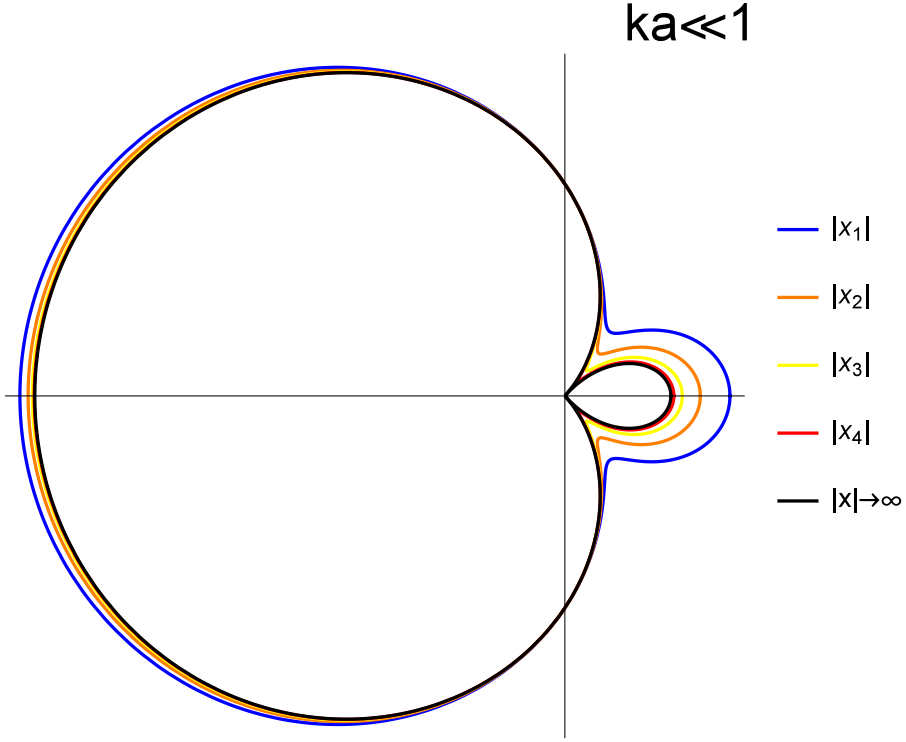


Figure 1. A sketch of the angular distribution of a plane wave scattered by a rigid sphere of radius a : $(\frac{d\sigma}{d\Omega})^{1/2}/a$ versus the polar angle θ for $ka \ll 1$ up to the f -wave contribution at different distances $|x_1| < |x_2| < |x_3| < |x_4| < |x|$.

The large-distance asymptotics then reads

$$P_{sc\infty}(\omega) \sim \frac{7\pi\rho_0\omega a^6 k^5}{9}. \quad (3.11)$$

This is just the result given by the conventional scattering theory [4].

4 Acoustic scattering on nonrigid sphere

In this section, we consider the problem of a plane wave scattering on a nonrigid sphere.

4.1 Scattering intensity

For a plane wave scattering on a nonrigid sphere, the phase shift δ_l can be obtained from the boundary condition of a nonrigid sphere [1, 4].

Inside a nonrigid sphere, the solution of the Helmholtz equation can be written as [1, 4]

$$u_e(\mathbf{x}) = i\omega\rho_e \sum_{l=0}^{\infty} A_l j_l(k_e |\mathbf{x}|) P_l(\cos\theta), \quad (4.1)$$

where $k_e = \omega/c_e$ with c_e the velocity of the acoustic wave inside the nonrigid sphere, ω the frequency of the acoustic wave, P_e the acoustic intensity inside the nonrigid sphere,

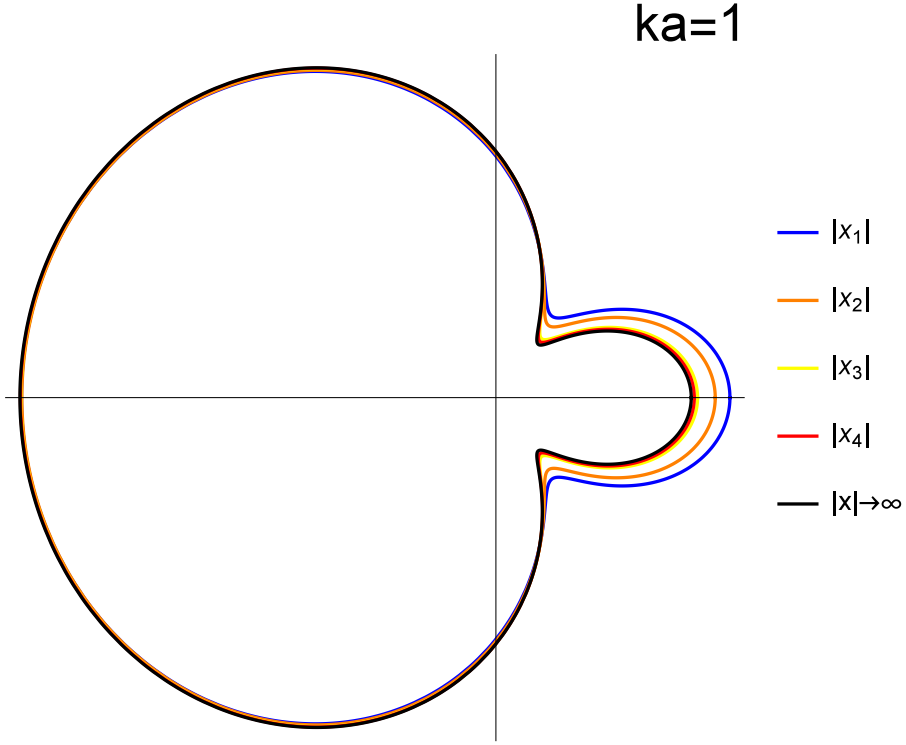


Figure 2. A sketch of the angular distribution of a plane wave scattered by a rigid sphere of radius a : $(\frac{d\sigma}{d\Omega})^{1/2}/a$ versus the polar angle θ for $ka = 1$ up to the f -wave contribution at different distances $|x_1| < |x_2| < |x_3| < |x_4| < |x|$.

and ρ_e the density of the nonrigid sphere. By Eq. (2.6) with $D_l = \frac{1}{4}i^l(2l+1)e^{2i\delta_l}$ and $C_l = \frac{1}{4}i^l(2l+1)$ [6], the solution $u_o(\mathbf{x})$ outside the sphere reads

$$u_o(\mathbf{x}) = \frac{i\omega\rho_0}{4} \sum_{l=0}^{\infty} i^l(2l+1) \left[h_l^{(2)}(k_0|\mathbf{x}|) + e^{2i\delta_l} h_l^{(1)}(k_0|\mathbf{x}|) \right] P_l(\cos\theta), \quad (4.2)$$

where $k_0 = \omega/c_0$, c_0 is the velocity of the acoustic wave outside the nonrigid sphere, and ρ_0 is the density outside the nonrigid sphere.

The phase shift δ_l is given by the connection condition on the boundary [1, 4]

$$u_e(\mathbf{x})|_{r=a} = u_o(\mathbf{x})|_{r=a}, \quad (4.3)$$

and

$$\frac{1}{i\omega\rho_\varepsilon} \frac{\partial}{\partial r} u_e(\mathbf{x}) \Big|_{r=a} = \frac{1}{i\omega\rho_0} \frac{\partial}{\partial r} u_o(\mathbf{x}) \Big|_{r=a}. \quad (4.4)$$

ka=2

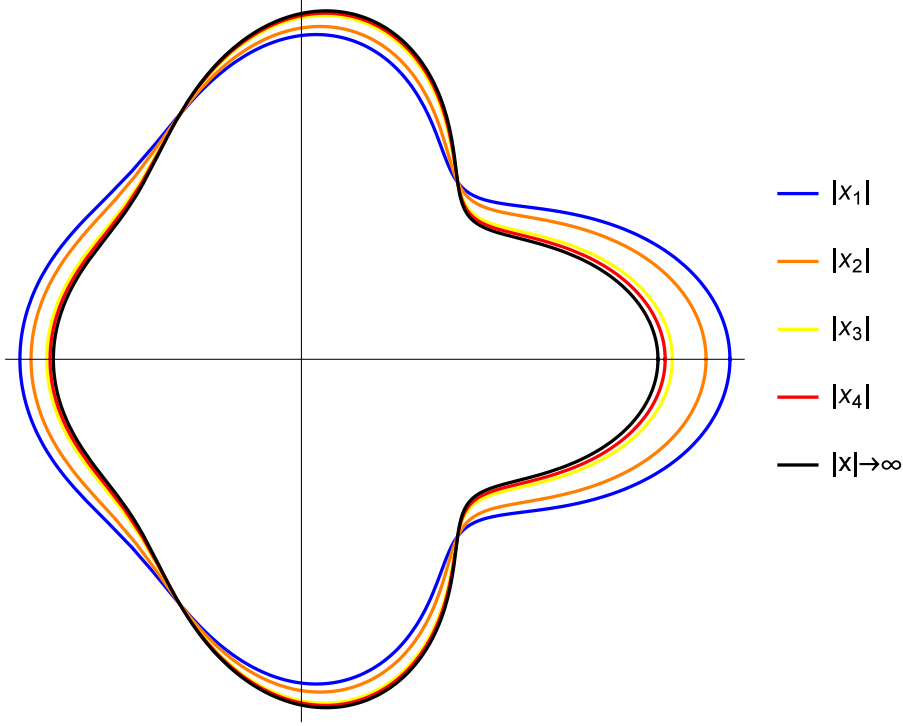


Figure 3. A sketch of the angular distribution of a plane wave scattered by a rigid sphere of radius a : $(\frac{d\sigma}{d\Omega})^{1/2}/a$ versus the polar angle θ for $ka = 2$ up to the f -wave contribution at different distances $|x_1| < |x_2| < |x_3| < |x_4| < |x|$.

Substituting Eqs. (4.1) and (4.2) into Eqs. (4.3) and (4.4) respectively gives

$$\begin{aligned}
 e^{2i\delta_l} &= \frac{\frac{\rho_e}{\rho_0} j_l(k_e r) \frac{dh_l^{(2)}(k_0 r)}{dr} - h_l^{(2)}(k_0 a) \frac{dj_l(k_e r)}{dr}}{h_l^{(1)}(k_0 r) \frac{d}{dr} j_l(k_e r) - \frac{\rho_e}{\rho_0} j_l(k_e r) \frac{dh_l^{(1)}(k_0 r)}{dr}} \Bigg|_{r=a} \\
 &= \frac{-j_l(k_e a) \left[l(\rho_0 - \rho_e) h_l^{(2)}(k_0 a) + ak_0 \rho_e h_{l+1}^{(2)}(k_0 a) \right] + ak_e \rho_0 h_l^{(2)}(k_0 a) j_{l+1}(k_e a)}{j_l(k_e a) \left[l(\rho_0 - \rho_e) h_l^{(1)}(k_0 a) + ak_0 \rho_e h_{l+1}^{(1)}(k_0 a) \right] - ak_e \rho_0 h_l^{(1)}(k_0 a) j_{l+1}(k_e a)},
 \end{aligned} \tag{4.5}$$

where $\frac{d}{dz} h_\nu^{(1,2)}(z) = \frac{\nu}{z} h_\nu^{(1,2)}(z) - h_{\nu+1}^{(1,2)}(z)$ and $\frac{d}{dz} j_\nu(z) = \frac{\nu}{z} j_\nu(z) - j_{\nu+1}(z)$ are used [24]. The phase shift then reads

$$\delta_l = \arg \left(j_l(k_e a) \left[l(\rho_0 - \rho_e) h_l^{(2)}(k_0 a) + ak_0 \rho_e h_{l+1}^{(2)}(k_0 a) \right] - ak_e \rho_0 h_l^{(2)}(k_0 a) j_{l+1}(k_e a) \right) - \frac{\pi}{2}. \tag{4.6}$$

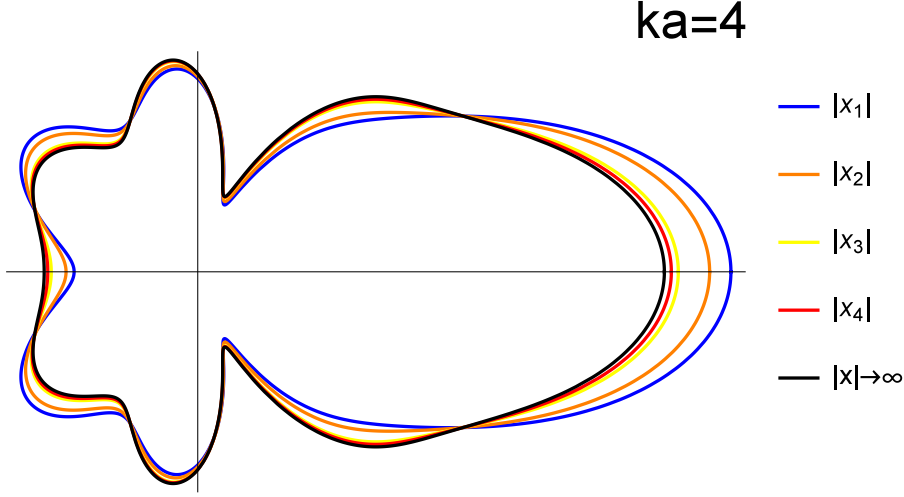


Figure 4. A sketch of the angular distribution of a plane wave scattered by a rigid sphere of radius a : $(\frac{d\sigma}{d\Omega})^{1/2}/a$ versus the polar angle θ for $ka = 4$ up to the f -wave contribution at different distances $|x_1| < |x_2| < |x_3| < |x_4| < |x|$.

Substituting Eq. (4.5) into Eq. (2.16) gives the scattering intensity,

$$I(\mathbf{x}) = \frac{\rho_0 \omega k_0}{|\mathbf{x}|^2} \left| \sum_{l=0}^{\infty} (2l+1) \frac{1}{2k_0} P_l(\cos \theta) y_l \left(\frac{i}{k_0 |\mathbf{x}|} \right) \times \left\{ \frac{2j_l(k_e a) [l(\rho_0 - \rho_e) j_l(k_0 a) + a k_0 \rho_e j_{l+1}(k_0 a)] - 2a k_e \rho_0 j_l(k_0 a) j_{l+1}(k_e a)}{j_l(k_e a) [l(\rho_0 - \rho_e) h_l^{(1)}(k_0 a) + a k_0 \rho_e h_{l+1}^{(1)}(k_0 a)] - a k_e \rho_0 h_l^{(1)}(k_0 a) j_{l+1}(k_e a)} \right\} \right|^2, \quad (4.7)$$

where $j_l(z) = \frac{1}{2} [h_l^{(2)}(z) + h_l^{(1)}(z)]$ is used [5].

Rayleigh scattering. Taking only the s -wave and p -wave contributions into account and assuming that $ka \ll 1$ gives the scattering intensity

$$I(\mathbf{x}) \sim \frac{\rho_0 \omega k_0^5 a^6}{9 |\mathbf{x}|^2} \left(\frac{\kappa_0 - \kappa_e}{\kappa_0} - 3 \frac{\rho_e - \rho_0}{2\rho_e + \rho_0} \cos \theta \right)^2 \times \left[1 + \left(\frac{2\rho_e + \rho_0}{\rho_e - \rho_0} \frac{\kappa_0 - \kappa_e}{3\kappa_0} \frac{1}{\cos \theta} - 1 \right)^{-2} \frac{1}{k_0^2 |\mathbf{x}|^2} \right], \quad (4.8)$$

where $\kappa_0 = k_0^2/\rho_0$ and $\kappa_e = k_e^2/\rho_e$.

When $|\mathbf{x}|$ tends to infinity, Eq. (4.8) reduces to

$$I_{\infty}(\mathbf{x}) \sim \frac{\rho_0 \omega k_0^5 a^6}{9 |\mathbf{x}|^2} \left[\frac{\kappa_0 - \kappa_e}{\kappa_0} - \frac{3(\rho_e - \rho_0)}{\rho_0 + 2\rho_e} \cos \theta \right]^2. \quad (4.9)$$

This is just the scattering intensity given by conventional scattering theory [1, 4].

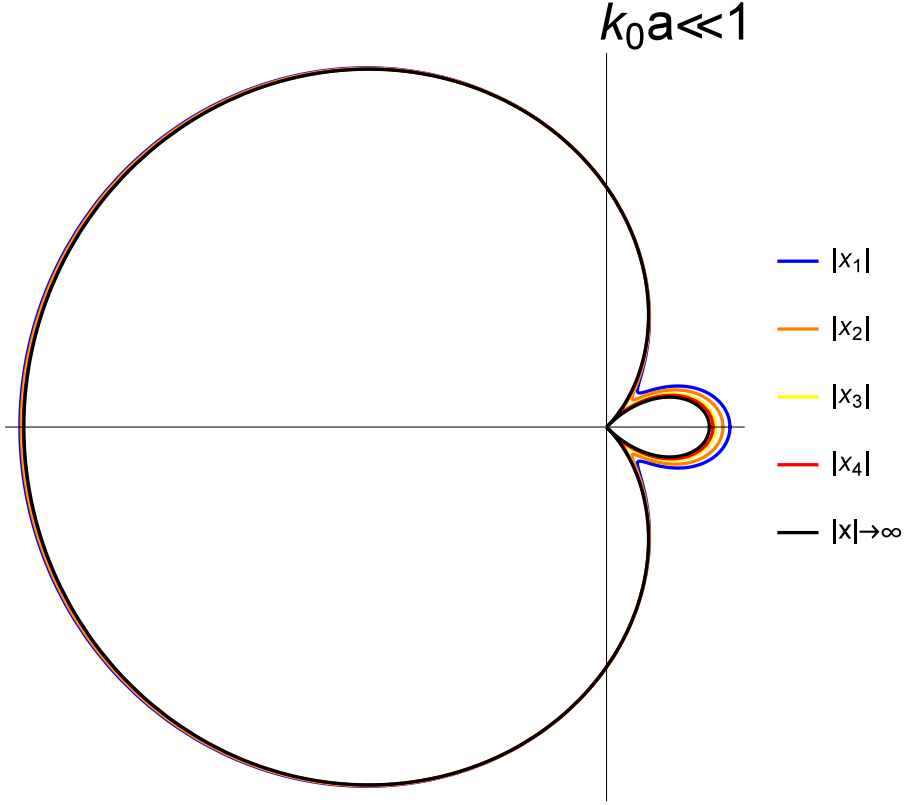


Figure 5. A sketch of the angular distribution of a plane wave scattered by a rigid sphere of radius a : $(\frac{d\sigma}{d\Omega})^{1/2}/a$ versus the polar angle θ for $k_0a \ll 1$ up to the f -wave contribution at different distance $|x_1| < |x_2| < |x_3| < |x_4| < |x|$.

4.2 Near target effect

In the following, we show the influence of the near target effect in scattering cross sections. Substituting $I(\mathbf{x})$ given by Eq. (4.7) into Eq. (3.7) gives the differential scattering cross section. In figures (5) to (8), we sketch $(\frac{d\sigma}{d\Omega})^{1/2}/a$ versus the polar angle θ at different distance $|x|$ for different wave lengths up to f -wave contribution.

In order to show the near target effect, we consider the deviation $\Delta\sigma = \sigma - \sigma_\infty$. By Eqs. (3.7), (4.8), and (4.9), we have

$$\frac{d\Delta\sigma}{d\Omega} = \frac{k_0^2 a^6}{9|\mathbf{x}|^2} \left(\frac{2\rho_e + \rho_0}{\rho_e - \rho_0} \frac{\kappa_0 - \kappa_e}{3\kappa_0} \frac{1}{\cos\theta} - 1 \right)^{-2}. \quad (4.10)$$

where we take only the s -wave and p -wave contributions into account and assume that $ka \ll 1$.

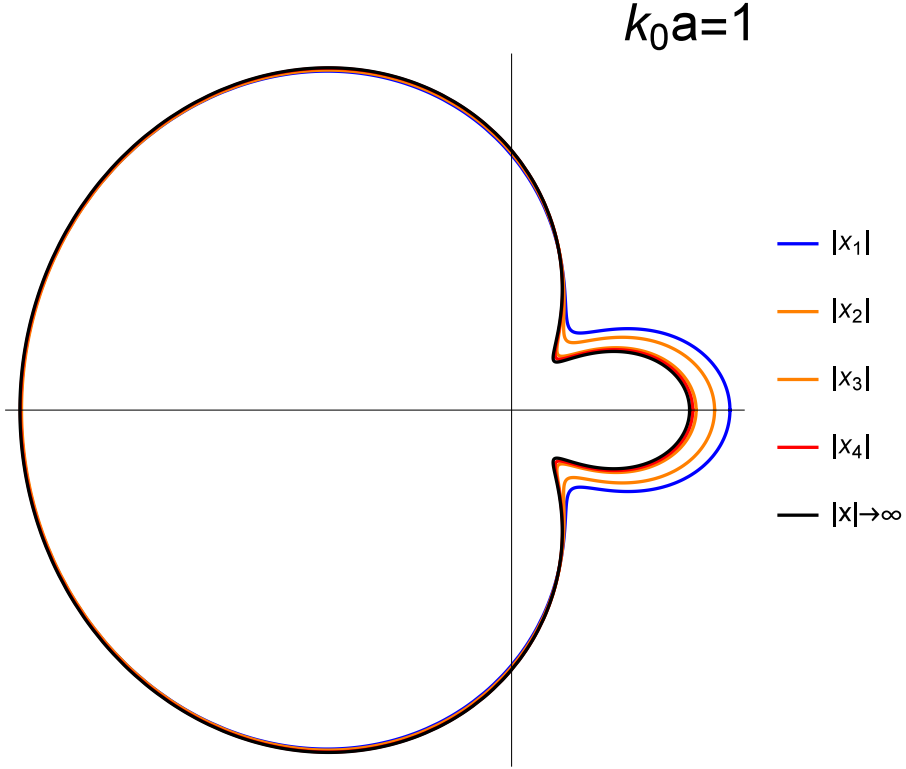


Figure 6. A sketch of the angular distribution of a plane wave scattered by a rigid sphere of radius a : $(\frac{d\sigma}{d\Omega})^{1/2}/a$ versus the polar angle θ for $k_0 a = 1$ up to the f -wave contribution at different distance $|x_1| < |x_2| < |x_3| < |x_4| < |x|$.

4.3 Power

The scattering power can be obtained by substituting Eq. (4.8) into Eq. (3.9).

$$P_{sc}(\omega, \mathbf{x}) \sim \frac{4\pi}{9} \rho_0 \omega k_0^5 a^6 \left[\frac{(\kappa_0 - \kappa_e)^2}{\kappa_0^2} + 3 \left(\frac{\rho_e - \rho_0}{2\rho_e + \rho_0} \right)^2 \left(1 + \frac{1}{k^2 |\mathbf{x}|^2} \right) \right]. \quad (4.11)$$

When $|\mathbf{x}|$ tends to infinity, Eq. (4.11) reduces to

$$P_{sc\infty}(\omega) \sim \frac{4\pi}{9} \rho_0 \omega k_0^5 a^6 \left[\frac{(\kappa_0 - \kappa_e)^2}{\kappa_0^2} + 3 \left(\frac{\rho_e - \rho_0}{2\rho_e + \rho_0} \right)^2 \right]. \quad (4.12)$$

This is just the scattering power given by the conventional scattering theory [1, 4].

5 Discussions and conclusion

In this paper, we provide a rigorous acoustic scattering theory without the large-distance asymptotic approximation. In our treatment, instead of the far-field pattern $u_\infty\left(\frac{\mathbf{x}}{|\mathbf{x}|}\right)$ in conventional scattering theory, we consider an exact pattern $u_{exact}(\mathbf{x})$ without the large-distance asymptotic approximation. The scattering intensity $I(\mathbf{x})$ is represented in terms

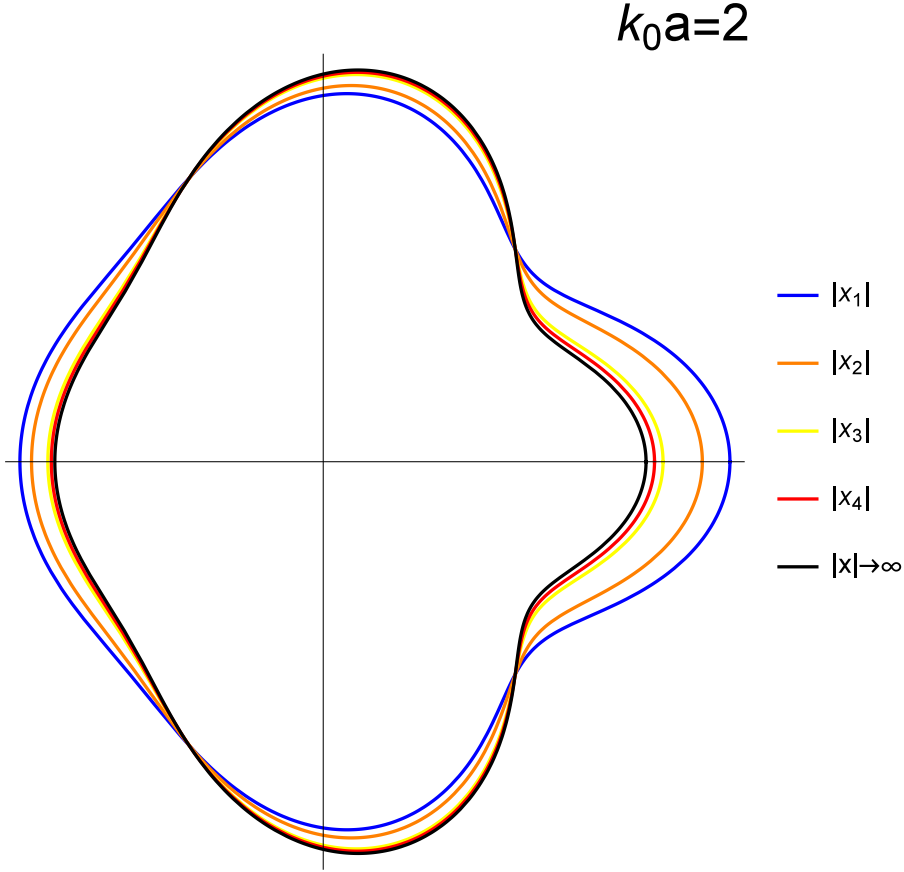


Figure 7. A sketch of the angular distribution of a plane wave scattered by a rigid sphere of radius a : $(\frac{d\sigma}{d\Omega})^{1/2}/a$ versus the polar angle θ for $k_0 a = 2$ up to the f -wave contribution at different distance $|x_1| < |x_2| < |x_3| < |x_4| < |x|$.

of the exact pattern $u_{exact}(\mathbf{x})$. The exact pattern $u_{exact}(\mathbf{x})$ is represented in terms of the phase shift δ_l . Two examples, plane waves scattering on a rigid sphere and on a nonrigid sphere are considered. We also compare our result with the result given by conventional scattering theory. Moreover, we show that the near target effect can not be ignored for long wavelength acoustic scattering.

In realistic acoustic scattering, the wavelength of acoustic waves is often comparable with the distance between target and observer. In this case, a rigorous theory of acoustic scattering that preserves the information of the distance becomes important.

In acoustic scattering, it is needed to calculate the scattering phase shift. The scattering phase shift is determined by solving the Helmholtz equation with the boundary condition on the obstacle. In further works, we can apply the heat-kernel method to calculate the scattering phase shift using the approach developed in Refs. [25–28].

In long wavelength scattering, such as the scattering of sounds with wavelength ranging from tens of centimeters to a few meters, sonars with wavelength ranging from tens of meters

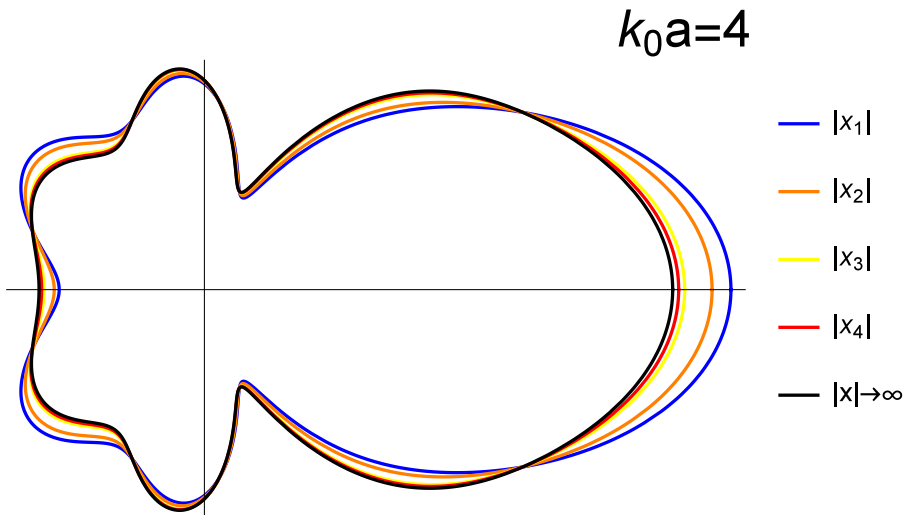


Figure 8. A sketch of the angular distribution of a plane wave scattered by a rigid sphere of radius a : $(\frac{d\sigma}{d\Omega})^{1/2}/a$ versus the polar angle θ for $k_0a = 4$ up to the f -wave contribution at different distance $|x_1| < |x_2| < |x_3| < |x_4| < |x|$.

to hundreds of meters, and earthquake waves with wavelength ranging from hundreds of meters to thousands of meters, the wavelength of acoustic waves is often too long to use the large-distance asymptotic approximation. In applications such as designing the structure of the theater, conducting deep sea and geological exploration by detecting the sonar and the earthquake wave, the distance is comparable with the wavelength in order to receive signals with enough intensity. Under this circumstance the near target effect needs to be reckoned in.

Acknowledgments

We are very indebted to Dr G. Zeitrauman for his encouragement. This work is supported in part by NSF of China under Grant No. 11575125 and No. 11675119.

References

- [1] P. M. Morse and K. U. Ingard, *Theoretical acoustics*. Princeton university press, 1968.
- [2] E. R. Pike and P. C. Sabatier, *Scattering, Two-Volume Set: Scattering and inverse scattering in Pure and Applied Science*. Academic press, 2001.
- [3] D. Colton and R. Kress, *Inverse Acoustic and Electromagnetic Scattering Theory*. Applied Mathematical Sciences. Springer, 1998.
- [4] M. Schroeder, *Handbook of Acoustics*. Springer, 2007.
- [5] T. Liu, W.-D. Li, and W.-S. Dai, *Scattering theory without large-distance asymptotics*, *Journal of High Energy Physics* **2014** (2014), no. 6 87.

- [6] W.-D. Li and W.-S. Dai, *Scattering theory without large-distance asymptotics in arbitrary dimensions*, *Journal of Physics A: Mathematical and Theoretical* **49** (2016), no. 46 465202.
- [7] J. D. González, E. F. Lavia, and S. Blanc, *A computational method to calculate the exact solution for acoustic scattering by fluid spheroids*, *Acta Acustica united with Acustica* **102** (2016), no. 6 1061–1071.
- [8] L. J. Ayton, *Acoustic scattering by a finite rigid plate with a poroelastic extension*, *Journal of Fluid Mechanics* **791** (2016) 414–438.
- [9] H. Jia, X. Li, and X. Meng, *Rigid and elastic acoustic scattering signal separation for underwater target*, *The Journal of the Acoustical Society of America* **142** (2017), no. 2 653–665.
- [10] Y. Chai, Z. Gong, W. Li, and T. Li, *Application of smoothed finite element method to acoustic scattering from underwater elastic objects*, *The Journal of the Acoustical Society of America* **141** (2017), no. 5 3708–3708.
- [11] P. D. Thorne, I. T. MacDonald, and C. E. Vincent, *Modelling acoustic scattering by suspended flocculating sediments*, *Continental Shelf Research* **88** (2014) 81–91.
- [12] A. Mantouka, H. Dogan, P. White, and T. Leighton, *Modelling acoustic scattering, sound speed, and attenuation in gassy soft marine sediments*, *The Journal of the Acoustical Society of America* **140** (2016), no. 1 274–282.
- [13] Y. Guo, D. Hömberg, G. Hu, J. Li, and H. Liu, *A time domain sampling method for inverse acoustic scattering problems*, *Journal of Computational Physics* **314** (2016) 647–660.
- [14] E. M. Fischell and H. Schmidt, *Supervised machine learning for estimation of target aspect angle from bistatic acoustic scattering*, *IEEE Journal of Oceanic Engineering* (2017).
- [15] A. Cavaleri, W. Wolf, and J. Jaworski, *Numerical solution of acoustic scattering by finite perforated elastic plates*, in *Proc. R. Soc. A*, vol. 472, p. 20150767, The Royal Society, 2016.
- [16] O. Steinbach and G. Unger, *Combined boundary integral equations for acoustic scattering-resonance problems*, *Mathematical Methods in the Applied Sciences* **40** (2017), no. 5 1516–1530.
- [17] C. Dutrion and F. Simon, *Acoustic scattering reduction using layers of elastic materials*, *Journal of Sound and Vibration* **388** (2017) 53–68.
- [18] M. Karimi, P. Croaker, N. Peake, and N. Kessissoglou, *Acoustic scattering for rotational and translational symmetric structures in nonuniform potential flow*, *AIAA Journal* (2017).
- [19] M. D. Guild, A. Alù, and M. R. Haberman, *Cloaking of an acoustic sensor using scattering cancellation*, *Applied Physics Letters* **105** (2014), no. 2 023510.
- [20] A. Merkel, G. Theocharis, O. Richoux, V. Romero-García, and V. Pagneux, *Control of acoustic absorption in one-dimensional scattering by resonant scatterers*, *Applied Physics Letters* **107** (2015), no. 24 244102.
- [21] G. T. Silva and H. Bruus, *Acoustic interaction forces between small particles in an ideal fluid*, *Physical Review E* **90** (2014), no. 6 063007.
- [22] F. Mitri, *Acoustic radiation force on a rigid elliptical cylinder in plane (quasi) standing waves*, *Journal of Applied Physics* **118** (2015), no. 21 214903.
- [23] V. Denis, A. Pelat, and F. Gautier, *Scattering effects induced by imperfections on an acoustic*

black hole placed at a structural waveguide termination, *Journal of Sound and Vibration* **362** (2016) 56–71.

- [24] F. W. Olver, *NIST handbook of mathematical functions hardback and CD-ROM*. Cambridge University Press, 2010.
- [25] N. Graham, M. Quandt, and H. Weigel, *Spectral methods in quantum field theory*, vol. 777. Springer, 2009.
- [26] A. Barvinsky and G. Vilkovisky, *Beyond the schwinger-dewitt technique: Converting loops into trees and in-in currents*, *Nuclear Physics B* **282** (1987) 163–188.
- [27] H. Pang, W.-S. Dai, and M. Xie, *Relation between heat kernel method and scattering spectral method*, *The European Physical Journal C* **72** (2012), no. 5 1–13.
- [28] W.-D. Li and W.-S. Dai, *Heat-kernel approach for scattering*, *The European Physical Journal C* **75** (2015), no. 6.